Common and distinct roles of frontal midline theta and occipital alpha oscillations in coding temporal intervals and spatial distances

Mingli Liang[1], Jingyi Zheng[2], Eve Isham[1], Arne Ekstrom[1]

[1]University of Arizona, [2]Auburn University

Abstract

Judging how far something is and how long it takes to get there are critical to memory and navigation. Yet, the neural codes for spatial and temporal information remain unclear, particularly how and whether neural oscillations might be important for such codes. To address these issues, participants traveled through teleporters in a virtual town while we simultaneously recorded scalp EEG. Participants judged the distance and time spent inside the teleporter. Our findings suggest that alpha power relates to distance judgments while frontal theta power relates to temporal judgments. In contrast, changes in alpha frequency and beta power indexed both spatial and temporal judgments. We also found evidence for fine-grained temporal coding and an effect of past trials on temporal but not spatial judgments. Together, these findings support partially independent coding schemes for spatial and temporal information, and suggest that low-frequency oscillations play important roles in coding both space and time.

Common and distinct roles of frontal midline theta and occipital alpha oscillations in coding temporal intervals and spatial distances

Introduction

Tracking where we are in space and time is important for both navigation and episodic memories (Eichenbaum & Cohen, 2014; Ekstrom & Isham, 2017; Robin & Moscovitch, 2014; Tulving, 2002). However, it is not clear what neural mechanisms are recruited for spatial and temporal coding in humans, and whether they share similar coding principles (Ekstrom & Isham, 2017; Frassinetti, Magnani, & Oliveri, 2009; Walsh, 2003). Movement induces robust hippocampal low-frequency oscillations (3-12Hz) in both rats (Vanderwolf, 1969) and humans (Bohbot, Copara, Gotman, & Ekstrom, 2017; Ekstrom et al., 2005; Goyal et al., 2020; Jacobs, 2013; Watrous, Fried, & Ekstrom, 2011). However, movement involves changes in both distance and time, and therefore, low-frequency oscillations might offer one potential mechanism reconciling spatial and temporal coding. To address these questions, it is important to decouple spatial and temporal information experimentally.

Theta oscillations are an important ingredient for spatial distance coding in humans. For example, hippocampal theta power increases linearly with the amount of distance traveled in VR (Bush et al., 2017; Vass et al., 2016). Further, cross-regional theta connectivity plays a critical role in judgments of relative spatial distance (Kim et al., 2018), and a distinctive role in differentiating distance from temporal contextual information (Watrous, Tandon, Conner, Pieters, & Ekstrom, 2013). Nonetheless, it is not clear if neocortical theta oscillations can code spatial distance in a similar fashion, and if scalp EEG is capable of revealing such a cortical theta distance code.

While past studies have provided some evidence for a role of low-frequency oscillations in spatial distance coding, their role in representing temporal intervals remains less clear. Some studies have looked at patterns of cortical low-frequency power when participants remember supra-second intervals. For example, the alpha-beta coupling strengths predict the precision of time reproduction (Grabot et al., 2019), and theta power in striatum and sensorimotor cortex discriminate rats' responses to

temporal interval comparisons (Gu, Kukreja, & Meck, 2018). Abundant evidence from single-unit recordings also suggests medial temporal lobe (MTL) structures form internally-generated assembly whose firing activities track time passage on scale of seconds (Itskov, Curto, Pastalkova, & Buzsáki, 2011; MacDonald, Lepage, Eden, & Eichenbaum, 2011; Pastalkova, Itskov, Amarasingham, & Buzsáki, 2008; Wang, Romani, Lustig, Leonardo, & Pastalkova, 2015). Given the prevalence of low-frequency oscillations in the human medial temporal lobe, it is possible that low-frequency power changes also relates to temporal interval coding.

Besides low-frequency power changes, another neocortical oscillatory mechanism of interval timing could relate to alpha frequency modulation, as suggested by (Cecere, Rees, & Romei, 2015; Samaha & Postle, 2015). Alpha frequency changes manifest independently of changes in alpha power (Samuel, Wang, Hu, & Ding, 2018), and this mechanism has been implicated in the temporal resolution of visual information in working memory (Cecere et al., 2015; Samaha & Postle, 2015). Specifically, slower occipital alpha impairs the perception of two temporally proximate stimuli (Samaha & Postle, 2015). Yet, how power and frequency fluctuations relate to interval timing remains largely unclear and unresolved.

In this current study, we examined how low-frequency oscillations uniquely support spatial distance and temporal interval coding, and whether they share similar coding schemes. To address these research questions, we developed a virtual navigation and teleportation task (Figure 1), based on the design from Vass et al. (2016). In this task, participants entered a virtual teleporter and were briefly presented with a blank screen, after which they exited the teleporter and were prompted to make a judgment regarding the distance transported or duration spent inside the teleporter. By manipulating the distance and duration independently, we disentangled participants' memory for spatial distance from that of temporal duration. This in turn allowed us to examine their neural correlates separately. In addition, participants physically walked in virtual reality by navigating on an omnidirectional treadmill while wearing a headmounted display, allowing us to study cortical oscillations under more ecologically

enriched conditions.

We tested three primary hypotheses. First, we tested whether cortical oscillatory power (2-30Hz) and occipital alpha frequency fluctuations contained sufficient information to support judgments of spatial distance and temporal intervals. Second, we tested whether such oscillatory codes differed for spatial distance vs. temporal interval judgments, which might further support the ideas of independent codes for spatial and temporal information (Watrous et al., 2013) vs. a common magnitude estimation mechanism (Walsh, 2003). Lastly, we tested whether neural representations for current judgments of time or distance were shaped by the information received during previous trials, given findings that amplitudes of ERPs related to interval timing are dependent on past trials (Wiener & Thompson, 2015), and that behavioral judgments of distance are influenced by the distance judged on past trials as well (Harootonian, Wilson, Hejtmánek, Ziskin, & Ekstrom, 2020). Together, these analyses allowed us to address to what extent the coding for spatial distance and temporal intervals involves common vs. distinct neural mechanisms.

Results

Longer intervals were associated with frontal midline theta and global beta power decreases

We first tested the hypothesis that cortical power fluctuations carry sufficient information to decode spatial distance traveled and temporal intervals estimated in the teleporter. We first tested the time code hypothesis (Figure 2A,D), beginning with testing whether cortical low-frequency power codes temporal intervals. We conducted electrode-by-electrode paired t-tests between power spectra for long vs. short temporal intervals trials. Results showed that long interval trials were associated with theta power decreases at Fz, FC1, F2, and beta power decreases at frontal and posterior sites (for theta power averaged across Fz, FC1 and F2, Cohen's $d = 0.12$, $M_{short} = 4.06$, $M_{long} = 4.02$, $SD_{short} = 0.33$, $SD_{long} = 0.34$, $t(18) = 5.46$, $p < 0.001$, 95% CI = [0.03, 0.06]; for beta power, Cohen's $d = 0.15$, $M_{short} = 4.44$, $M_{long} = 4.40$, $SD_{short} = 0.27$,

SD_{long} = 0.27, t(18) = 6.72, p < 0.001, 95% CI = [0.03, 0.06]). These findings support a role for theta and beta power decreases in coding temporal intervals.

To further confirm the role of frontal midline theta oscillations in interval timing, we employed a binary classifier (see Time-frequency analysis methods) to decode types of temporal intervals in the teleporter (Figure 2F). Results confirmed that we could successfully classify short interval from the 4-8 s portion of the long interval trials using frontal midline theta power (M = 79.35%, SD = 7.43%, t(18) = 17.22, p < 0.001, 95% CI = [75.77%, 82.93%]). However, the same classifier did not successfully decode the distance traveled in the teleporter, suggesting the specificity of frontal midline theta in supporting temporal interval coding (M = 46.16%, SD = 6.15%, t(18) = -2.72, p = 0.01, 95% CI = [43.20%, 49.13%]). As an additional control analysis, we trained the same classifier with frontal theta power to discriminate the 0-4s portion of long interval trials from the short interval trials. This served as a control because participants could not have known what types of intervals they experienced until they crossed the 4s threshold. Indeed, the classifier was not able to decode whether the trials were short interval trials (4s) or the 0-4s portion of long interval trials (M = 45.86%, SD = 4.42%, t(18) = -4.09, p < 0.001, 95% CI = [43.73%, 47.98%]). Together, these findings support a unique role for frontal midline theta oscillations in coding temporal intervals but not spatial distance.

Longer distances traveled were linked to decreases in alpha and beta power

We further tested the hypothesis that power fluctuations would contain sufficient information for spatial distance traveled in the teleporter (Figure 2B,E). We found lower delta power for short distance vs. long distance at the following electrode sites: FP1, F7, AF7 (for delta power averaged, Cohen's d = 0.10, M_{short} = 5.25, M_{long} = 5.27, SD_{short} = 0.21, SD_{long} = 0.21, t(18) = -3.15, uncorrected p = 0.001, 95% CI = [-0.03 -0.01]). We also found higher alpha power for shorter distance at the following sites: Pz, CP2, Cz, F8, P2, CPz, CP4, FC4 and FT8 (for alpha power averaged, Cohen's d = 0.09, M_{short} = 4.99, M_{long} = 4.96, SD_{short} = 0.35, SD_{long} = 0.33, t(18) = 2.38,

uncorrected p = 0.03, 95% CI = [0.00,0.04]). We also found widespread beta power increases for short distance teleportation (Cohen's d = 0.08, M_{short} = 4.57, M_{long} = 4.55, SD_{short} = 0.26, SD_{long} = 0.26, t(18) = 4.42, uncorrected p < 0.001, 95% CI = [0.01, 0.02]). Given that no electrode-wise power contrasts for distance codes survived FDR multiple comparison correction, as an assay for their robustness, we used binomial tests to test how consistent the power effects were among participants. Although the effects of lower delta power were not consistent across participants (14/19, p = 0.06), alpha and beta power increases for short distance trials were consistent (alpha: 15/19, p = 0.01, beta: 16/19, p = 0.004). These findings support a possible role for alpha power changes in spatial distance coding.

To further test whether judgments of spatial distances and temporal intervals involved distinct patterns of power fluctuations, power differences between short and long trials were analyzed with a 2 (Task: spatial distance vs. temporal intervals) × 3 (Frequency bands: theta, alpha and beta) between-subject ANOVA. If spatial and temporal judgments involved distinct sets of oscillatory signatures, we would expect to see an interaction between Task and Frequency. As predicted, the interaction between Task and Frequency was significant, $F(2, 108) = 11.09$, $MSE = 0.00$, $p < .001$, $\hat{\eta}^2_G = .170$ (Table 1).

Alpha frequency modulation: a common mechanism for spatial and temporal judgments

We suspected that occipital alpha frequency modulation could be an additional form of distance and time coding in our teleportation task, as suggested by (Cao & Händel, 2019; Samaha & Postle, 2015). To test this idea, we compared the peak frequency of alpha oscillations at occipital sites for short vs. long distance trials. Results revealed that occipital alpha oscillations were of higher frequency for short distance trials compared to long distance trials (collapsed across occipital electrodes and trials, Cohen's d = 0.13, M_{short} = 10.32Hz, M_{long} = 10.28Hz, SD_{short} = 0.30, SD_{long} = 0.30, t(18) = 5.13, p < 0.001, 95% CI = [0.03,0.06], Figure 3A,B).

Occipital alpha frequency also varied between short and long temporal interval trials. Occipital alpha frequency was faster for short interval trials than the 4-8s portion of long interval trials (Cohen's $d = 0.73$, $M_{short} = 10.32$Hz, $M_{4-8sLong} = 10.11$Hz, $SD_{short} = 0.25$, $SD_{4-8sLong} = 0.32$, $t(18) = 5.90$, $p < 0.001$, 95% CI = [0.13,0.28], Figure 3A). As a control analysis, we also compared occipital alpha frequency for short interval trials and the 0-4s portion of long interval trials; the alpha frequencies did not differ ($M_{short} = 10.32$Hz, $M_{0-4sLong} = 10.31$Hz, $SD_{short} = 0.25$, $SD_{0-4sLong} = 0.23$, $t(18) = 0.55$, $p = 0.59$, 95% CI = [-0.03,0.05], Figure 3A).

Earlier, we reported that between short vs. long distance trials, alpha power at central electrodes differed weakly. We speculate that the weak alpha power differences related in part to frequency differences. Therefore we examined alpha frequency at sites Pz, CP2, Cz, P2, CPz, CP4. Alpha at the six electrode sites oscillated at higher frequencies for short distance traversals than long distance ones (Cohen's $d = 0.15$, $M_{short} = 10.22$Hz, $M_{long} = 10.18$Hz, $SD_{short} = 0.28$, $SD_{long} = 0.27$, $t(18) = 4.40$, $p < 0.001$, 95% CI = [0.02,0.07]). Together, these findings support alpha frequency modulation as a shared mechanism for coding spatial distance and temporal intervals.

Fine-scaled, continuous-like temporal information could be decoded from scalp EEG signals

We proceeded to ask whether temporal interval codes might be present in the EEG data at a finer scale, inspired by Bright et al. (2019), for example, at the level of milliseconds (Figure 4). We trained classifiers on 2-30Hz power to decode time passage at the scale of 100ms/250ms (see classification analyses methods), and we were able to decode continuous-like temporal information from short interval trials at a performance significantly above chance (M = 12.64%, SD = 2.05%, chance level = 1/16 = 6.25%, one sample t-test $t(18) = 13.33$, $p < 0.001$, 95% CI = [11.63%, 13.64%]), from long interval trials (M = 5.94%, SD = 0.81%, chance level = 1/32 = 3.13%, one sample t-test $t(18) = 14.70$, $p < 0.001$, 95% CI = [5.54%, 6.34%]), and from the distance teleportation trials as well (M = 9.37%, SD = 0.91%, chance level = 1/22 = 4.55%, one

sample t-test t(18) = 22.39, p <0.001, 95% CI = [8.92%, 9.83%]). These findings suggest the intriguing possibility that more fine-scaled, continuous-like temporal codes could be embedded in low-frequency oscillations, regardless of the specific task.

We note that following entry into the teleporter, participants exhibited a P300-like ERP response (Polich, 2007) at Cz electrode (see Figure 6). Therefore we repeated the fine-scaled time classification analyses, with the grand P300 averaged component subtracted for every trial. After removing the P300 responses, we were still able to successfully decode continuous-like temporal information from the short interval trials (M = 5.92%, SD = 1.08%, chance level = 1/40 = 2.50%, one sample t-test t(18) = 13.75, p <0.001, 95% CI = [5.39%, 6.44%]), from the long interval trials (M = 3.04%, SD = 0.91%, chance level = 1/80 = 1.60%, one sample t-test t(18) = 8.60, p <0.001, 95% CI = [2.61%, 3.48%]), and from the distance trials (M = 3.92%, SD = 0.36%, chance level = 1/56 = 1.79%, one sample t-test t(18) = 25.84, p <0.001, 95% CI = [3.74%, 4.09%]). Lastly, to further exclude the possible contribution of movement-related noise and other unidentified ERPs in early onsets of a trial, we removed the first second of teleportation epochs and repeated the fine-scaled time classification analyses. We were again able to successfully decode continuous-like time information from short interval trials above chance (M = 3.96%, SD = 0.46%, chance level = 1/30 = 3.33%, one sample t-test t(18) = 5.88, p <0.001, 95% CI = [3.73%, 4.18%]), from long interval trials (M = 1.78%, SD = 0.27%, chance level = 1/70 = 1.43%, one sample t-test t(18) = 5.80, p <0.001, 95% CI = [1.65%, 1.91%]), and from distance trials above chance as well (M = 2.84%, SD = 0.22%, chance level = 1/46 = 2.17%, one sample t-test t(18) = 13.22, p <0.001, 95% CI = [2.73%, 2.94%]).

Memory effects: Past trials influenced frontal theta and occipital alpha codes for judging temporal intervals but not spatial distances.

Finally, we tested the hypothesis that past trials might exert an influence on temporal and spatial judgments of current trials. Hereafter we abbreviate short trials with a previous short trial to S_S, short trials with a previous long trial to S_L, long trials

with a previous short trial to L_S, and long trials with a previous long trial to L_L. As stated in methods (see representation similarity analysis methods and Figure 5A,B), if memory effects were absent for the neural codes of short interval trials, then we would predict an equality among the following three indices of similarity: similarity within S_S, similarity within S_L, and cross similarity between S_S and S_L. If memory effects were present for short interval trials, we would predict an inequality among those three similarity indices. To test whether frontal theta codes and occipital alpha codes would show memory effects independent of each other, we conducted the memory-effect analyses here independently for both sets of features. P values reported in this section were Bonferroni-corrected.

We first tested the existence of memory effects for temporal interval trials. Frontal theta power codes for short interval trials showed memory effects (Figure 5D, inequality was found, within simS_S > sim*Cross*, t(18) = 3.35, p = 0.01, and within simS_L > sim*Cross*, t(18) = 3.79, p = 0.003). Occipital alpha power codes also showed memory effects for short interval trials (Figure 5D, inequality was found, within simS_S > sim*Cross*, t(18) = 3.90, p = 0.003, and simS_L > sim*Cross*, t(18) = 4.93, p < 0.001). These findings suggest the presence of memory effects for short interval trials, for both their frontal theta and occipital alpha code.

However, 4-8s portions of long interval trials did not show memory effects, regardless of whether the neural codes were assessed by frontal theta or occipital alpha power. No memory effects were found for the frontal theta codes of 4-8s portions from long interval trials (Figure 5C, equality was found, simL_S = sim*Cross*, t(18) = 0.38, p = 1, and simL_L = sim*Cross*, t(18) = -1.10, p = 0.87). Occipital alpha power codes for long interval trials (4-8s) did not show memory effects either (Figure 5C, equality was found, simL_S = sim*Cross*, t(18) = 0.70, p = 1, and simL_L = sim*Cross*, t(18) = -1.49, p = 0.45). These findings together suggest that past trial memories did not influence the front-midline theta nor occipital alpha representations for long interval trials (4-8s).

We further confirmed that no memory effects were found for spatial distance trials. Frontal theta power codes for spatial trials did not show memory effects from

past trials (no memory effects for short distance trials, simS_S = sim*Cross*, t(18) = -0.90, p = 1, simS$_L$ = sim*Cross*, t(18) = -0.03, p = 1; no memory effects for long distance trials, simL$_S$ = sim*Cross*, t(18) = -0.47, p = 1; simL$_L$ = sim*Cross*, t(18) = -0.47, p = 1). No memory effects were discovered either for the occipital alpha power codes of spatial distance trials (no memory effects for short distance trials, simS$_S$ = sim*Cross*, t(18) = -2.4, p = 0.09, simS$_L$ = sim*Cross*, t(18) = 0.04, p = 1; no memory effects were found for long distance trials, simL$_S$ = sim*Cross*, t(18) = 1.35, p = 0.57, simL$_L$ = sim*Cross*, t(18) = -0.88, p = 1). Together, these findings suggest that the memory effects were specific to temporal judgments, but not distance judgments.

Discussion

In the current study, we tested whether semi-periodic fluctuations recorded at the scalp supported coding for spatial distance and temporal duration. Decades of research support a role for low-frequency oscillations, both in cortex and hippocampus, in coding movement speed during navigation (Jacobs, 2013; McFarland, Teitelbaum, & Hedges, 1975; Vanderwolf, 1969; Watrous et al., 2011). To attempt to disentangle space and time, which are strongly intertwined in movement speed, participants experienced teleportation of different spatial distance and temporal intervals in the absence of any optic flow or other sensory input to provide cues about speed, similar to the design in Vass et al. (2016). Results from time-frequency analyses suggest a potential role of central-occipital alpha power and global beta power for distance coding, and a role of frontal theta and global beta power changes for time coding. Furthermore, the frequency-sliding analyses (Cohen, 2014) indicate that changes in occipital alpha frequency coded both long vs. short distance trials and long vs. short temporal interval trials, suggesting frequency modulation as a potential common mechanism for spatial and temporal coding. Classifiers trained on power spectra further support the hypothesis that temporal information could be decoded from scalp EEG signals, both at a coarse (long vs. short) and fine scale (100 or 250ms). Finally, our representation similarity analyses indicate that frontal theta and occipital alpha power codes for

temporal intervals were influenced by past trials, suggesting a memory effect for temporal interval judgments.

Our results supporting a role for cortical theta power in temporal but not spatial coding have important implications. One of our hypotheses was that frontal midline theta power coded distance traveled in the teleporter, given that hippocampal delta and theta power linearly coded the distance traveled (Bush et al., 2017; Vass et al., 2016), and that in rodents prefrontal theta are coupled with hippocampal oscillations during mobility (Siapas, Lubenov, & Wilson, 2005; Young & McNaughton, 2009). In contrast, in the current study we did not find a robust association between cortical theta power and distance coding, but rather cortical alpha and beta power coded short and long distance trials. We offer three interpretations here on the null findings linking cortical theta and spatial distance coding. One possibility is that prefrontal theta oscillations are phase locked but not amplitude locked to hippocampal theta (Young & McNaughton, 2009), and therefore phase information in frontal theta but not power changes code spatial distance or temporal interval (see Watrous et al., 2013, for an example of this). This is an issue we cannot address in the current study because scalp EEG does not give reliable access to hippocampal signals. A second possibility is that prefrontal theta may be locked to the temporal-processing or memory-related components, but not the movement-related components, of hippocampal(HPC) theta oscillations (Goyal et al., 2020; Watrous et al., 2013), as supported by our findings of frontal theta power changes during temporal, but not spatial trials. A third possibility is that HPC movement-related theta (3-12 Hz) oscillations manifest in the cortex within the traditional alpha band (8-12Hz) consistent with the alpha band we observed for spatial distance judgments. The third interpretation is consistent with recent arguments (Aghajan et al., 2017; Bohbot et al., 2017; Goyal et al., 2020) suggesting that HPC movement-related theta oscillations, particularly during real-world movements, manifest most prominently above 8Hz, which would align with the frequency range of traditional alpha band (8-12 Hz) rather than theta band (4-8 Hz).

Our findings of a double dissociation between distance-related alpha power

changes and time-related frontal theta power changes provide further evidence for partially independent codes for space and time in the human brain. A similar double dissociation between distance-related alpha power and time-related frontal beta power has also been reported using an encode-reproduction paradigm (Robinson & Wiener, 2020). Occipital alpha oscillations often manifest during navigation paradigms, perhaps consistent with its visually enriched nature in humans (Ekstrom, 2015), and occipital alpha oscillations support the visuospatial processes involved (such as optic flow, Cao & Händel, 2019). As proposed by Goyal et al. (2020), a theoretical link might exist between HPC movement-related theta and occipital alpha oscillations. For example, eye closure induces alpha power increases both at occipital sites and in hippocampus (Geller et al., 2014). Our current results would suggest differing roles in navigation for frontal midline theta (4-8 Hz) and occipital alpha (8-12 Hz), which were both found relevant to movement (Liang, Starrett, & Ekstrom, 2018), and frontal midline theta and occipital alpha oscillations can cooperate to support task-dependent spatial or temporal processing. Therefore, a helpful next step would be to determine how these signals coordinate between hippocampus and cortex in our task using ECoG.

One of our novel findings involves demonstrating a more general role of alpha frequency modulation in supporting both temporal and spatial judgments. Specifically for the temporal task, we found faster occipital alpha for shorter distance traveled, and slower occipital alpha during the 4-8s portions of long interval trials vs. short interval trials. What roles could endogenous alpha frequency modulation possibly play here? One explanation is the processing-speed theory, where occipital alpha frequency indexes the processing speed of incoming sensory information (Klimesch, Doppelmayr, Schimke, & Pachinger, 1996). We speculate that the sensory processing speed differed between short and long interval trials because of their different cognitive demands. To complete the temporal task, participants only needed to track time passage in the teleporter up to 4s, and not beyond 4s, and therefore the cognitive demands differed between 0-4s and 4-8s portions of the temporal task. This processing-speed view is supported by findings from Samuel et al. (2018) showing that occipital alpha frequency was correlated with

working memory loads in a working memory task.

In contrast to the processing-speed account, however, an alternative interpretation of alpha frequency modulation is that alpha plays more than a binary role in distinguishing temporal intervals, given that we could decode fine-scaled and continuous-like temporal information from 2-30 Hz power of scalp EEG signals. Instead we suggest a perceptual resolution account, and speculate that the occipital alpha frequency could causally determine the resolution of suprasecond temporal perception: for example, individuals with 10 Hz resting occipital alpha oscillations can discriminate two temporal intervals with a minimum of 100ms (1/10) differences, and those with 12 Hz resting alpha could discriminate two intervals with 83.33ms minimal differences (1/12). This perceptual resolution account is also suggested by Samaha and Postle (2015) showing that occipital alpha frequency reflects the "refresh rate" of visual perception and occipital alpha represents the perceptual unit of temporal processing (Cecere et al., 2015). Consistent with this view, we predict that occipital alpha frequency should affect not only the encoding but also the retrieval and reproduction of temporal intervals, given that tACS-induced shifts in resting alpha frequency lead to shifts in subjective time experiences (Mioni et al., 2020), alpha-beta phase amplitude coupling correlates with time reproduction precision (Grabot et al., 2019), and that alpha frequency is central to the strengths of alpha-beta coupling. Future studies could investigate how interval reproduction performance is associated with alpha frequency modulation in healthy humans, as well as in the pre-clinical Alzheimer populations which show irregularities in parietal alpha oscillations (Montez et al., 2009).

Given that we found alpha frequency modulation and beta power fluctuations related to both spatial and temporal judgments, our results provide evidence for a common mechanism for spatial and temporal coding involving magnitude estimation. Although distance-related beta power has rarely been studied in a scalp EEG setting, the timing-related beta power we observed has been noted in predicting the accuracy and precision of time production (Grabot et al., 2019; Kononowicz & van Rijn, 2015; Robinson & Wiener, 2020). Our findings suggest that beta oscillations may reflect a

common magnitude representation underlying both spatial and temporal processing, and that such distance and continuous-like temporal information could be widely accessible in neocortical regions, including early sensory and motor cortices. Future studies can bridge the gap of research between spatial and temporal processing, and further elaborate the roles of beta oscillations in spatial coding vs. temporal coding, with a variety of tasks such as estimating and reproducing spatial distance with a path integration task (Harootonian et al., 2020).

Another finding in our study was the effect of past trials on neural codes related to temporal but not spatial judgments, suggesting a partial dissociation between spatial and temporal processing. The memory effects of past perceptual history on interval timing is predicted under the framework of Scalar Timing Theory (Gibbon & Church, 2014; Van Rijn, Gu, & Meck, 2014), which proposes that to perceive a currently ongoing interval, a ratio comparison is needed between a previously exposed interval and the pacemaker outcomes of the currently perceived interval. Our findings of the memory-dependent aspect of time perception is also well aligned with similar findings based on ERP analyses (Wiener & Thompson, 2015). For spatial distance judgments, we found null memory effects related to their neural representations, despite some reports of such memory effects at a behavioral level (Harootonian et al., 2020). Notably, this could be because in our task, prior to the start of teleportation, participants could immediately judge spatial distance based on the locations of entrances of the teleportation, and in contrast, the temporal judgment required continuous tracking throughout the 0-4s to discriminate short from long intervals. Therefore, our findings suggest that spatial distance judgments, at least in our task, may mostly be contingent upon currently available visual information while temporal judgments may necessitate references to past perceptual information and comparisons between current sensory input and past mnemonic output.

Conclusions

Our study addressed an important issue regarding whether spatial and temporal processing share common or distinct mechanisms (Eichenbaum & Cohen, 2014; Ekstrom, Copara, Isham, Wang, & Yonelinas, 2011; Frassinetti et al., 2009; Gauthier, Pestke, & Van Wassenhove, 2019; Gauthier, Prabhu, Kotegar, & van Wassenhove, 2020; Watrous et al., 2013; Wiener & Thompson, 2015). Our findings suggest two manners in which spatial and temporal judgments differ during navigation: the first is that as a function of power changes within specific frequency bands, temporal judgments resulted in changes in cortical theta and beta power, while spatial judgments resulted in changes in cortical alpha and beta power. Second, we found that oscillatory codes for temporal judgments were influenced by past trials while such codes for spatial judgments were not. Consistent with the idea of separable representations for space and time, spatial and temporal discounting are behaviorally distinctive from each other (Robinson, Michaelis, Thompson, & Wiener, 2019), estimating spatial distance can be subject to large errors (Zhao, 2018) while estimating suprasecond intervals can be performed with relatively high accuracy (Grabot et al., 2019), and spatial and temporal estimation errors distort in opposing manners (Brunec, Javadi, Zisch, & Spiers, 2017). The dissociation between space and time are also supported at the level of oscillatory signatures. For example, theta oscillations are crucial for both time and space coding, but with subtle nuances. Hippocampal theta oscillations code generally for movement, and one suggestion is that they involve two functionally distinct components dissociable by space and time (Watrous et al., 2013) related to anterior vs. posterior hippocampus (Goyal et al., 2020). Therefore, evidence exists for and against the notion that space and time processing are of the same nature, and we also found evidence for alpha frequency and beta power modulation as common mechanisms for spatial and temporal coding. Thus, one implication of our study is that there are both distinct and common mechanisms related to how we process spatial distance and temporal intervals.

Acknowledgements

We thank Stephanie Doner for the assistance in scalp EEG data collection, Eva Robinson for feedbacks on the manuscript, and the participants for being part of this study.

Methods and Materials

Participants

Nineteen healthy adults (seven females) were recruited from the Tucson community in the study and received monetary and/or class credit for compensation. Consent was obtained in accordance with the Institutional Review Board at the University of Arizona. Prior to testing, participants performed a virtual reality training session to screen out those with susceptibility to cybersickness.

Virtual Environment

The virtual environment was constructed with the Unity Engine and rendered with an HTC Vive headset, and immersive walking experiences were simulated with an omnidirectional treadmill (KAT VR Gaming Pro, KAT VR, Hangzhou China, Figure 1B). The layout of the virtual environment was a plus (+) sign (Figure 1A), with four arms extending from the center. Four target stores were placed at the end of each arm. The teleporters were spawned in front of the target store for each trial, and upon entry, participants exited at the center of the plus maze.

Behavioral tasks

Participants completed two tasks: spatial distance task and temporal interval task. In the spatial task, the teleporters displaced the participants with one of the two possible spatial distance while the temporal interval was kept constant. In the temporal task, participants stayed in the teleporter and view a black screen for either a short or long duration before being transported to the center of plus maze for a fixed distance.

The sequential order of the two tasks were counterbalanced across participants. Each task involved 48 trials.

At the beginning of the first trial of the task, participants navigated to a given target store, and when arrived a teleporter spawned in front of the store. Upon entering the teleporter, participants view a black screen for a few seconds and then they were transported to the center of the plus maze. After exiting the teleporter, they were given instructions to decide which target store to visit next. For the spatial task, instructions were: "If far distance, go find store A. If short distance, go find store B." For the temporal task, instructions were: "If long interval, go find store A. If short interval, go find store B." By asking participants to judge spatial distance and temporal intervals, we ensured that they coded these two task-relevant variables.

For the spatial task, the duration of viewing black screen was kept constant, 5.656 seconds (Figure 1C). Long distance was defined as 200 virtual units and short distance was 100 virtual units. For the temporal task, the distance traveled was kept constant, 141.4 virtual units. The long temporal interval was defined as 8s of viewing a black screen while the short interval was 4s (Figure 1D). The order of long/short trials were pseudorandomized. Before starting the main experiment, participants were shown three long/short examples or until the participants reported understanding the differences between long/short trials.

EEG recording and preprocessing

Scalp EEG was recorded with a 64-channel ActiCAP system and was wirelessly transmitted through a MOVE module (BrainVision LLC, Morrisville, NC). Impedances of electrodes were kept below 5kΩ before proceeding. Preprocessing and analyses were performed with MATLAB, EEGLAB (Makeig, Debener, Onton, & Delorme, 2004), and customized codes. A 1-50Hz bandpass filter and artifact subspace reconstruction was applied to the raw continuous data, before extracting epochs aligned with the starts and ends of teleportation.

For the spatial task, we ran independent component analysis (ICA) on the

epoched data with SAISCA (a semi-automatic independent component rejection procedure, Chaumon, Bishop, and Busch (2015)) to aid artifact rejection. On average 19.42 components were rejected (SD = 6.08). For the temporal task, epoched long interval trials and short interval trials were first concatenated together as a "continuous" data structure, before ICA was performed on the concatenated data. On average 35.32 components were rejected (SD = 10.81). The ICA procedure for the temporal task was different because EEGLAB currently does not support a structure housing trials with inconsistent length. By concatenating 4s and 8s trials, we ensured trials of both types received identical ICA cleaning standards.

Time-frequency analysis

Power. We estimated the instantaneous power with 6-cycle Morlet Wavelets using codes from Hughes, Whitten, Caplan, and Dickson (2012). We sampled frequencies from 2 to 30 Hz in 20 logarithmic frequency steps. Multiple electrode-wise power spectra comparisons were implemented with FDR multiple-comparison corrected, q = 0.05 (Benjamini & Yekutieli, 2001). For the distance teleportation trials, 256 paired t-tests were corrected, and none of them were significant (critical p = 0). For the time teleportation task, 256 paired t-tests were corrected, and 54 were significant (critical p = 0.0015).

Instantaneous frequencies. We used frequency sliding (Cohen, 2014) to estimate the instantaneous frequency fluctuations. We first used a plateau 8-12Hz bandpass filter with 15% transition zone on the preprocessed EEG data. We employed the Hilbert Transform to extract the phase angle series. Prefiltered instantaneous frequencies at each timepoint t were estimated as the angular velocity,

$$f(t) = (\phi(t) - \phi(t-1)) * \frac{s}{2\pi} \tag{1}$$

where f is the instantaneous estimate of frequency, ϕ is the phase angle series, t is the timepoint of interest, and s is the EEG sampling rate. Then, we applied a 10th order median filter to the frequency series. We dropped the frequency estimates for the first 100ms and last 100ms for every trial, to ameliorate edge artifacts. We specifically

looked at the alpha frequencies at occipital sites (Pz,P3, P7, O1, Oz, O2, P4, P8, P1, P5, PO7, PO3, POz, PO4, PO8, P6, P2, Iz).

Classification analyses

To confirm the role of frontal theta power in temporal judgments, we constructed binary classifiers with the random forest algorithm (Wright & Ziegler, 2017) in R (R Core Team, 2018), with parameters set to default, except for the number of trees to 300. We used frontal theta power as features: three electrodes showing statistical theta power differences for the temporal task were selected (Fz, FC1, and F2), and their theta power values were used to train classifiers (4.08Hz, 4.70Hz, 5.42Hz, 6.26Hz and 7.21Hz).

To examine whether fine-scaled and continuous-like time codes were present in the scalp EEG signal, we built the following multiclass classifier to decode time based on 2-30 Hz power. We grouped instantaneous power series into multiple timebins. Power estimates within each timebin were averaged, and the resulting power spectra of 64 electrodes for each timebin were features used for classifiers. For our initial attempt, we used a timebin size of 250ms, and the SVM algorithm (*fitcecoc* from MATLAB, with coding style as *one vs all*), 33% of data as testing set, and 60 times for total iterations per participant. For the attempts with P300 removed and first second removed, we used a bin size of 100ms, and used the random forest algorithm; 33% of data were preserved as testing set and we set the number of iterations to 100 per participant.

Representation similarity analysis

In this analysis, we examined how past trials influenced the neural signals related to current judgments. For the purpose of simplicity, we abbreviate short trials with a previous short trial to S_S, short trials with a previous long trial to S_L, long trials with a previous short trial to L_S, and long trials with a previous long trial to L_L.

To test the hypothesis of whether neural codes differed for judgments with different previous trials, for example, whether neural codes differed between S_S and S_L, we evaluated the following three types of similarity indices (see Figure 5A,B):

1. pairwise similarity within S_S: the averaged similarity for all possible pairs within trials S_S,

2. pairwise similarity withinS_L: the averaged similarity for all possible pairs within trials S_L,

3. pairwise similarity across S_S and S_L: the averaged similarity for all possible pairs between trials S_S and S_L.

When no memory effects are present for the neural codes of short interval trials, it is predicted that three similarity indices are exactly equal to each other. When memory effects are present, inequality among those three similarity indices (specifically, $1 \neq 3$ and $2 \neq 3$) would be predicted.

To evaluate the similarity of two epochs, we calculated the Pearson correlation of their instantaneous power series, and transformed the coefficients into Fisher's Z-scores. To test whether frontal theta codes and occipital alpha codes would show memory effects independently, we selected the two following sets of features based on findings from power spectra analyses:

1. instantaneous theta power time series (4.08, 4.70, 5.42, 6.25 and 7.21Hz) at electrodes Fz, FC1, F2;

2. instantaneous alpha power time series (8.32, 9.59, 11.06 Hz) at occipital sites (Pz,P3, P7, O1, Oz, O2, P4, P8, P1, P5, PO7, PO3, POz, PO4, PO8, P6, P2, Iz).

Data availability

The data sets collected and analyzed during this study are available on `https://osf.io/3vxkn/`.

References

Aghajan, Z. M., Schuette, P., Fields, T. A., Tran, M. E., Siddiqui, S. M., Hasulak, N. R., ... et al. (2017, Dec). Theta oscillations in the human medial temporal lobe during real-world ambulatory movement. *Current Biology*, *27*(24), 3743-3751.e3. doi: https://doi.org/10.1016/j.cub.2017.10.062

Benjamini, Y., & Yekutieli, D. (2001). The control of the false discovery rate in multiple testing under dependency. *Annals of statistics*, 1165–1188.

Bohbot, V. D., Copara, M. S., Gotman, J., & Ekstrom, A. D. (2017). Low-frequency theta oscillations in the human hippocampus during real-world and virtual navigation. *Nature communications*, *8*(1), 1–7. doi: https://doi.org/10.1038/ncomms14415

Bright, I. M., Meister, M. L., Cruzado, N. A., Tiganj, Z., Howard, M. W., & Buffalo, E. A. (2019). A temporal record of the past with a spectrum of time constants in the monkey entorhinal cortex. *bioRxiv*, 688341. doi: https://doi.org/10.1101/688341

Brunec, I. K., Javadi, A.-H., Zisch, F. E. L., & Spiers, H. J. (2017, Sep). Contracted time and expanded space: The impact of circumnavigation on judgements of space and time. *Cognition*, *166*, 425–432. doi: https://doi.org/10.1016/j.cognition.2017.06.004

Bush, D., Bisby, J. A., Bird, C. M., Gollwitzer, S., Rodionov, R., Diehl, B., ... Burgess, N. (2017). Human hippocampal theta power indicates movement onset and distance travelled. *Proceedings of the National Academy of Sciences of the United States of America*, *114*(46), 12297–12302. doi: https://doi.org/10.1073/pnas.1708716114

Cao, L., & Händel, B. (2019). Walking enhances peripheral visual processing in humans. *PLoS biology*, *17*(10), e3000511. doi: https://doi.org/10.1371/journal.pbio.3000511.g003

Cecere, R., Rees, G., & Romei, V. (2015). Individual differences in alpha frequency drive crossmodal illusory perception. *Current Biology*, *25*(2), 231–235. doi:

https://doi.org/10.1016/j.cub.2014.11.034

Chaumon, M., Bishop, D. V., & Busch, N. A. (2015). A practical guide to the selection of independent components of the electroencephalogram for artifact correction. *Journal of neuroscience methods*, *250*, 47–63. doi: https://doi.org/10.1016/j.jneumeth.2015.02.025

Cohen, M. X. (2014). Fluctuations in oscillation frequency control spike timing and coordinate neural networks. *Journal of Neuroscience*, *34*(27), 8988–8998. doi: https://doi.org/10.1523/JNEUROSCI.0261-14.2014

Eichenbaum, H., & Cohen, N. J. (2014). Can We Reconcile the Declarative Memory and Spatial Navigation Views on Hippocampal Function? *Neuron*, *83*(4), 764–770. doi: https://doi.org/10.1016/j.neuron.2014.07.032

Ekstrom, A. D. (2015). Why vision is important to how we navigate. *Hippocampus*, *25*(6), 731–735. doi: https://doi.org/10.1002/hipo.22449

Ekstrom, A. D., Caplan, J. B., Ho, E., Shattuck, K., Fried, I., & Kahana, M. J. (2005). Human hippocampal theta activity during virtual navigation. *Hippocampus*, *15*(7), 881–889. doi: https://doi.org/10.1002/hipo.20109

Ekstrom, A. D., Copara, M. S., Isham, E. A., Wang, W.-c., & Yonelinas, A. P. (2011, Jun). Dissociable networks involved in spatial and temporal order source retrieval. *NeuroImage*, *56*(3), 1803–1813. doi: https://doi.org/10.1016/j.neuroimage.2011.02.033

Ekstrom, A. D., & Isham, E. A. (2017). Human spatial navigation: representations across dimensions and scales. *Current Opinion in Behavioral Sciences*, *17*, 84–89. doi: https://doi.org/10.1016/j.cobeha.2017.06.005

Frassinetti, F., Magnani, B., & Oliveri, M. (2009). Prismatic lenses shift time perception. *Psychological Science*, *20*(8), 949–954. doi: https://doi.org/10.1111/j.1467-9280.2009.02390.x

Gauthier, B., Pestke, K., & Van Wassenhove, V. (2019). Building the arrow of time.. over time: A sequence of brain activity mapping imagined events in time and space. *Cerebral Cortex*, *29*(10), 4398–4414. doi:

https://doi.org/10.1093/cercor/bhy320

Gauthier, B., Prabhu, P., Kotegar, K. A., & van Wassenhove, V. (2020). Hippocampal Contribution to Ordinal Psychological Time in the Human Brain. *Journal of Cognitive Neuroscience*, 1–15. doi: https://doi.org/10.1162/jocn_a_01586

Geller, A. S., Burke, J. F., Sperling, M. R., Sharan, A. D., Litt, B., Baltuch, G. H., ... Kahana, M. J. (2014). Eye closure causes widespread low-frequency power increase and focal gamma attenuation in the human electrocorticogram. *Clinical Neurophysiology*, *125*(9), 1764–1773. doi: https://doi.org/10.1016/j.clinph.2014.01.021

Gibbon, J., & Church, R. M. (2014). 26 sources of variance in an information processing theory of timing. *Animal cognition*, *1*, 465.

Goyal, A., Miller, J., Qasim, S. E., Watrous, A. J., Zhang, H., Stein, J. M., ... Jacobs, J. (2020). Functionally distinct high and low theta oscillations in the human hippocampus. *Nature Communications*, *11*(1), 498055. doi: https://doi.org/10.1038/s41467-020-15670-6

Grabot, L., Kononowicz, T. W., Dupré la Tour, T., Gramfort, A., Doyère, V., & van Wassenhove, V. (2019). The strength of alpha-beta oscillatory coupling predicts motor timing precision. *The Journal of Neuroscience*, *39*(17), 2473–18. doi: https://doi.org/10.1523/JNEUROSCI.2473-18.2018

Gu, B. M., Kukreja, K., & Meck, W. H. (2018). Oscillation patterns of local field potentials in the dorsal striatum and sensorimotor cortex during the encoding, maintenance, and decision stages for the ordinal comparison of sub- and supra-second signal durations. *Neurobiology of Learning and Memory*, *153*(May), 79–91. doi: https://doi.org/10.1016/j.nlm.2018.05.003

Harootonian, S. K., Wilson, R. C., Hejtmánek, L., Ziskin, E. M., & Ekstrom, A. D. (2020). Path integration in large-scale space and with novel geometries: Comparing vector addition and encoding-error models. *PLoS Computational Biology*, *16*(5), 1–27. doi: https://doi.org/10.1371/journal.pcbi.1007489

Hughes, A. M., Whitten, T. A., Caplan, J. B., & Dickson, C. T. (2012). BOSC: A

better oscillation detection method, extracts both sustained and transient rhythms from rat hippocampal recordings. *Hippocampus*, *22*(6), 1417–1428. doi: https://doi.org/10.1002/hipo.20979

Itskov, V., Curto, C., Pastalkova, E., & Buzsáki, G. (2011). Cell assembly sequences arising from spike threshold adaptation keep track of time in the hippocampus. *Journal of Neuroscience*, *31*(8), 2828–2834. doi: https://doi.org/10.1523/JNEUROSCI.3773-10.2011

Jacobs, J. (2013). Hippocampal theta oscillations are slower in humans than in rodents: implications for models of spatial navigation and memory. *Philosophical Transactions of the Royal Society B: Biological Sciences*, *369*(1635), 20130304–20130304. doi: 10.1098/rstb.2013.0304

Kim, K., Schedlbauer, A., Rollo, M., Karunakaran, S., Ekstrom, A. D., & Tandon, N. (2018, Jan). Network-based brain stimulation selectively impairs spatial retrieval. *Brain Stimulation*, *11*(1), 213–221. doi: https://doi.org/10.1016/j.brs.2017.09.016

Klimesch, W., Doppelmayr, M., Schimke, H., & Pachinger, T. (1996). Alpha frequency, reaction time, and the speed of processing information. *Journal of Clinical Neurophysiology*. doi: https://doi.org/10.1097/00004691-199611000-00006

Kononowicz, T. W., & van Rijn, H. (2015). Single trial beta oscillations index time estimation. *Neuropsychologia*, *75*, 381–389. doi: https://doi.org/10.1016/j.neuropsychologia.2015.06.014

Liang, M., Starrett, M. J., & Ekstrom, A. D. (2018). Dissociation of frontal-midline delta-theta and posterior alpha oscillations: A mobile EEG study. *Psychophysiology*(January), e13090. doi: https://doi.org/10.1111/psyp.13090

MacDonald, C. J., Lepage, K. Q., Eden, U. T., & Eichenbaum, H. (2011). Hippocampal "time cells" bridge the gap in memory for discontiguous events. *Neuron*, *71*(4), 737–749. doi: https://doi.org/10.1016/j.neuron.2011.07.012

Makeig, S., Debener, S., Onton, J., & Delorme, A. (2004). Mining event-related brain dynamics. *Trends in cognitive sciences*, *8*(5), 204–210. doi:

https://doi.org/10.1016/j.tics.2004.03.008

McFarland, W. L., Teitelbaum, H., & Hedges, E. K. (1975, Jan). Relationship between hippocampal theta activity and running speed in the rat. *Journal of Comparative and Physiological Psychology*, *88*(1), 324–328. doi: https://doi.org/10.1037/h0076177

Mioni, G., Shelp, A., Stanfield-Wiswell, C., Gladhill, K. A., Bader, F., & Wiener, M. (2020). Modulation of individual alpha frequency with tacs shifts time perception. *bioRxiv*. doi: https://doi.org/10.1101/2020.07.23.218230

Montez, T., Poil, S.-S., Jones, B. F., Manshanden, I., Verbunt, J. P. A., van Dijk, B. W., ... Linkenkaer-Hansen, K. (2009). Altered temporal correlations in parietal alpha and prefrontal theta oscillations in early-stage Alzheimer disease. *Proceedings of the National Academy of Sciences*, *106*(5), 1614–1619. doi: https://doi.org/10.1073/pnas.0811699106

Pastalkova, E., Itskov, V., Amarasingham, A., & Buzsáki, G. (2008). Internally generated cell assembly sequences in the rat hippocampus. *Science*, *321*(5894), 1322–1327. doi: https://doi.org/10.1126/science.1159775

Polich, J. (2007). Updating p300: an integrative theory of p3a and p3b. *Clinical neurophysiology*, *118*(10), 2128–2148. doi: https://doi.org/10.1016/j.clinph.2007.04.019

R Core Team. (2018). R: A language and environment for statistical computing [Computer software manual]. Vienna, Austria. Retrieved from `https://www.R-project.org/`

Robin, J., & Moscovitch, M. (2014). The effects of spatial contextual familiarity on remembered scenes, episodic memories, and imagined future events. *Journal of Experimental Psychology: Learning, Memory, and Cognition*, *40*(2), 459–475. doi: https://doi.org/10.1037/a0034886

Robinson, E. M., Michaelis, K., Thompson, J. C., & Wiener, M. (2019). Temporal and spatial discounting are distinct in humans. *Cognition*, *190*, 212–220. doi: https://doi.org/10.1016/j.cognition.2019.04.030

Robinson, E. M., & Wiener, M. (2020). Separable neural indices for time and distance estimation during path integration. *bioRxiv*. doi: https://doi.org/10.1101/2020.05.23.110882

Samaha, J., & Postle, B. R. (2015). The Speed of Alpha-Band Oscillations Predicts the Temporal Resolution of Visual Perception. *Current Biology*, *25*(22), 2985–2990. doi: https://doi.org/10.1016/j.cub.2015.10.007

Samuel, I. B. H., Wang, C., Hu, Z., & Ding, M. (2018). The frequency of alpha oscillations: task-dependent modulation and its functional significance. *Neuroimage*, *183*, 897–906. doi: https://doi.org/10.1016/j.neuroimage.2018.08.063

Siapas, A. G., Lubenov, E. V., & Wilson, M. A. (2005, apr). Prefrontal phase locking to hippocampal theta oscillations. *Neuron*, *46*(1), 141–151. doi: https://doi.org/10.1016/j.neuron.2005.02.028

Tulving, E. (2002). Episodic memory: from mind to brain. *Annu Rev Psychol*, *53*, 1–25. doi: https://doi.org/10.1146/annurev.psych.53.100901.135114

Vanderwolf, C. H. (1969). Hippocampal electrical activity and voluntary movement in the rat. *Electroencephalography and clinical neurophysiology*, *26*(4), 407–418. doi: https://doi.org/10.1016/0013-4694(69)90092-3

Van Rijn, H., Gu, B.-M., & Meck, W. H. (2014). Dedicated clock/timing-circuit theories of time perception and timed performance. In *Neurobiology of interval timing* (pp. 75–99). Springer.

Vass, L. K., Copara, M. S., Seyal, M., Shahlaie, K., Farias, S. T., Shen, P. Y., & Ekstrom, A. D. (2016). Oscillations Go the Distance: Low-Frequency Human Hippocampal Oscillations Code Spatial Distance in the Absence of Sensory Cues during Teleportation. *Neuron*, *89*(6), 1180–1186. doi: https://doi.org/10.1016/j.neuron.2016.01.045

Walsh, V. (2003). A theory of magnitude: Common cortical metrics of time, space and quantity. *Trends in Cognitive Sciences*, *7*(11), 483–488. doi: https://doi.org/10.1016/j.tics.2003.09.002

Wang, Y., Romani, S., Lustig, B., Leonardo, A., & Pastalkova, E. (2015). Theta sequences are essential for internally generated hippocampal firing fields. *Nature Neuroscience*, *18*(2), 282–288. doi: https://doi.org/10.1038/nn.3904

Watrous, A. J., Fried, I., & Ekstrom, A. D. (2011). Behavioral correlates of human hippocampal delta and theta oscillations during navigation. *Journal of Neurophysiology*, *105*(4), 1747–1755. doi: https://doi.org/10.1152/jn.00921.2010.

Watrous, A. J., Tandon, N., Conner, C. R., Pieters, T., & Ekstrom, A. D. (2013). Frequency-specific network connectivity increases underlie accurate spatiotemporal memory retrieval. *Nature Neuroscience*, *16*(3), 349–356. doi: https://doi.org/10.1038/nn.3315

Wiener, M., & Thompson, J. C. (2015). Repetition enhancement and memory effects for duration. *NeuroImage*, *113*, 268–278. doi: https://doi.org/10.1016/j.neuroimage.2015.03.054

Wright, M. N., & Ziegler, A. (2017). ranger: A fast implementation of random forests for high dimensional data in C++ and R. *Journal of Statistical Software*, *77*(1), 1–17. doi: https://doi.org/10.18637/jss.v077.i01

Young, C. K., & McNaughton, N. (2009, jan). Coupling of theta oscillations between anterior and posterior midline cortex and with the hippocampus in freely behaving rats. *Cerebral Cortex*, *19*(1), 24–40. doi: https://doi.org/10.1093/cercor/bhn055

Zhao, M. (2018). Human spatial representation: What we cannot learn from the studies of rodent navigation. *Journal of Neurophysiology*, *120*(5), 2453–2465. doi: https://doi.org/10.1152/jn.00781.2017

Table 1

tasks (space vs. time) and frequency bands (delta, theta, alpha, and beta) two way ANOVA test on the power differences between short and long trials.

Effect	F	df_1	df_2	MSE	p	$\hat{\eta}^2_G$
Freq.	5.12	2	108	0.00	.007	.087
Task demands	1.68	1	108	0.00	.198	.015
Freq. $\times$ Task	11.09	2	108	0.00	$< .001$	.170

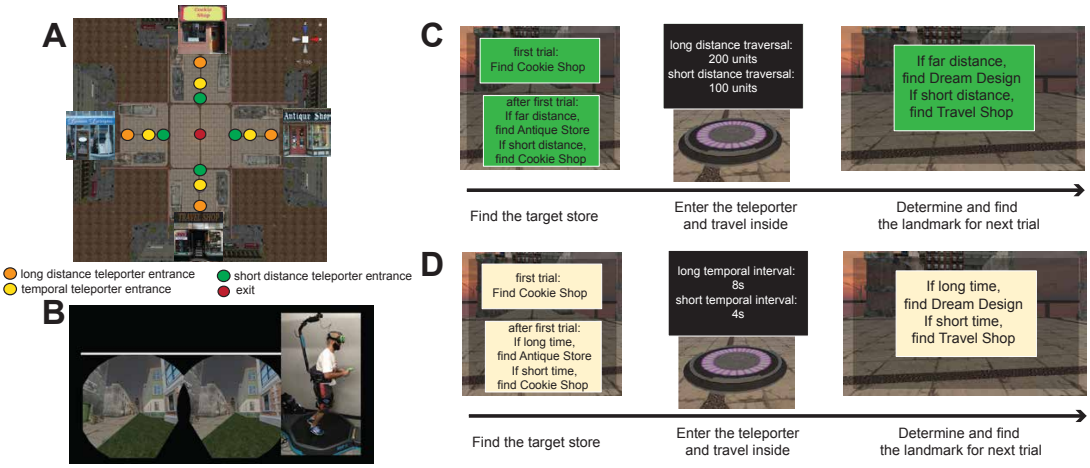

Figure 1. Spatial and temporal tasks, and virtual reality setup. **(a)** Bird view of the virtual plus maze. Orange, green and yellow dots mark possible teleporter entrances. **(b)** Demonstration of the KATVR omnidirectional treadmill and HTC Vive headset. **(c)** Spatial task. **(d)** Temporal task.

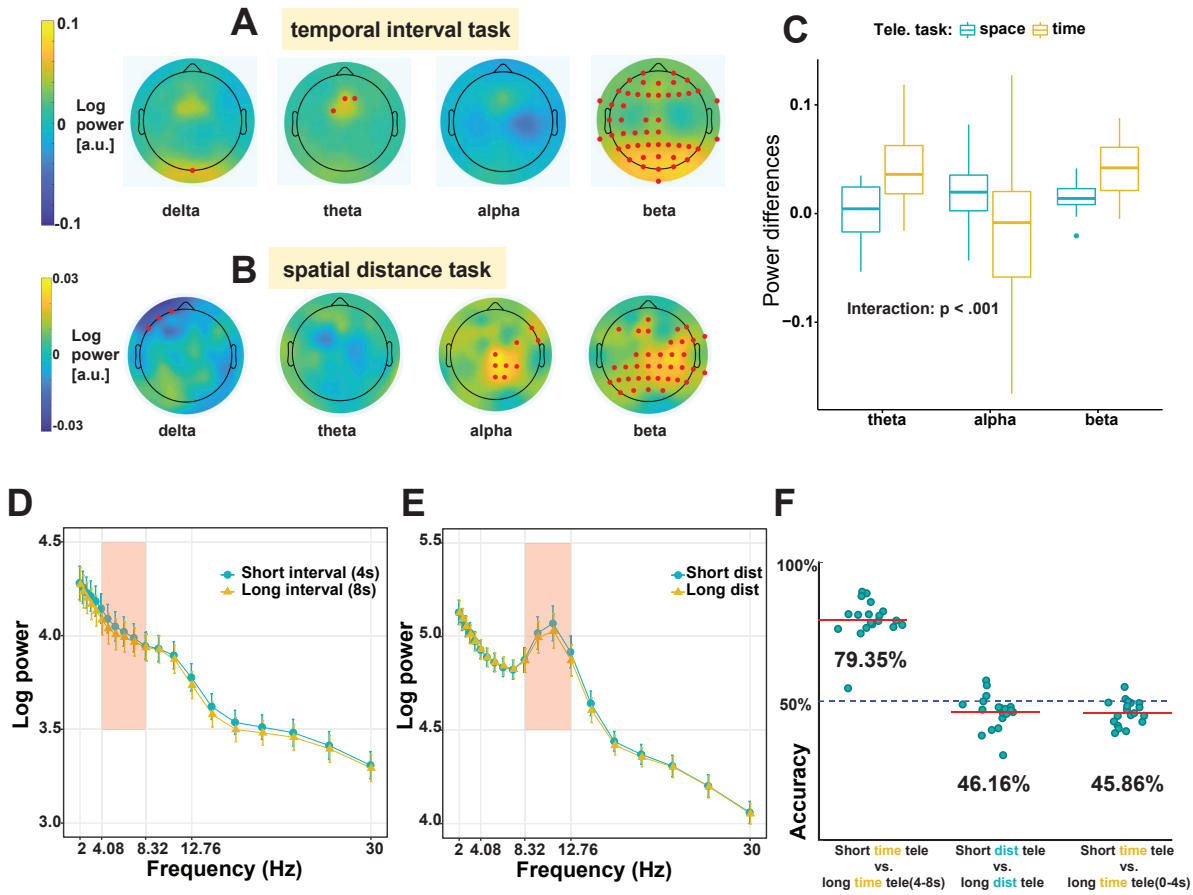

Figure 2. Experiencing different spatial distance and temporal intervals in a teleporter was linked to changes in power at distinct frequencies. **(a)** Longer intervals are linked to frontal midline theta and global beta power decreases. Red dots mark electrodes showing statistical significance. **(b)** Longer distances traveled were linked with decreases in alpha and beta power. Please note that comparisons for spatial distance are uncorrected for multiple comparisons (see main text). **(c)** Box plots for power differences between short and long trials for space and time task. Medians are represented by the lines at the center of boxes. The significant interaction between tasks × frequency bands supports partially independent coding for spatial and temporal judgments. **(d)** Power spectra averaged within electrodes Fz,FC1,F2 showing higher theta power for short interval trials. **(e)** Power spectra averaged within central-posterior electrodes showing higher alpha power for short distance trials. Error bars in (d,e) represent standard errors. **(f)** With frontal theta power as features, trial types in the temporal task but not in the spatial task could be successfully decoded.

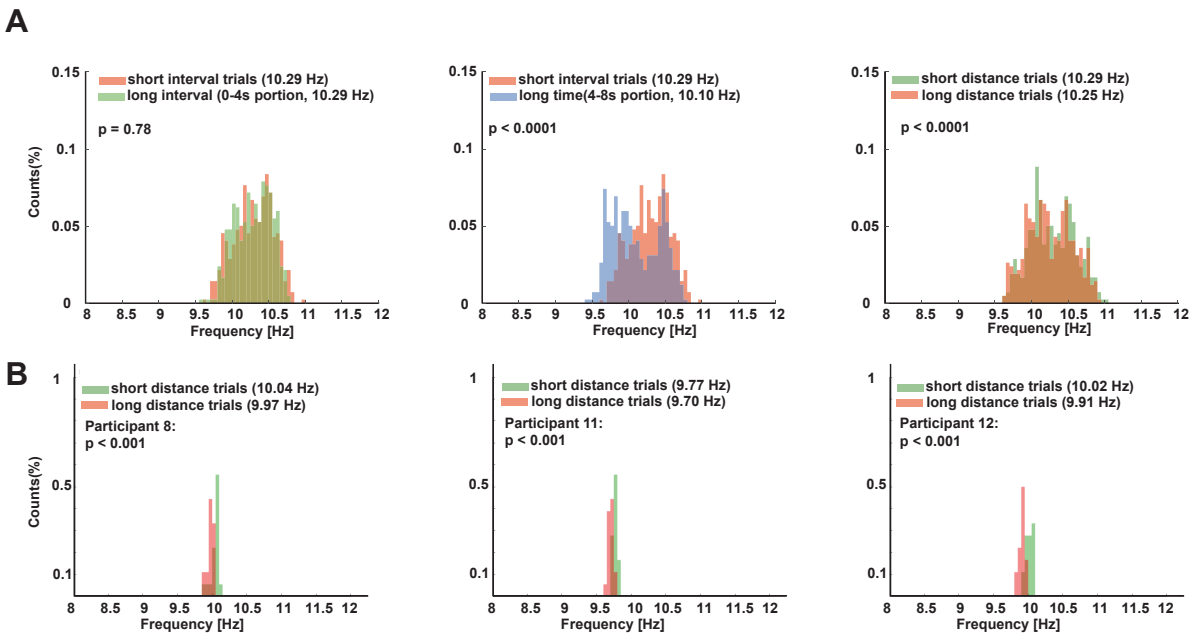

Figure 3. Occipital alpha frequency modulation as a potential shared mechanism for both spatial distance and temporal interval judgments. **(a)** Drawn from all participants, distributions of alpha frequency per electrode, averaged across trials and time. Faster occipital alpha frequency was seen for short vs. long distance trials, and for short vs. long interval (4-8s portion) trials. **(b)** Distributions of occipital alpha frequency for distance task from three example participants, averaged across trials and time.

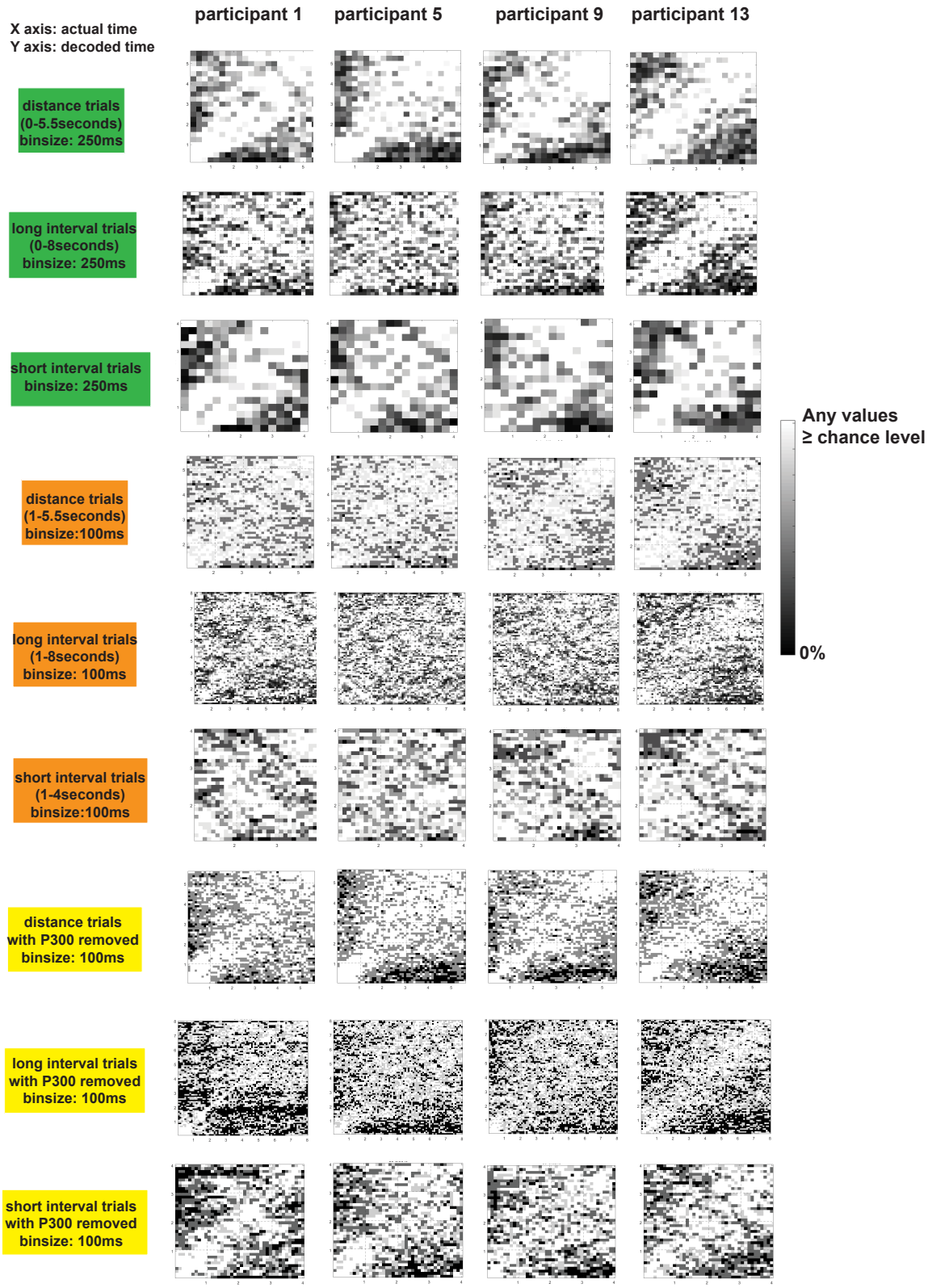

Figure 4. Fine-grained temporal information can be decoded from scalp EEG broadband power. Decoding outputs from four example participants are shown here. Gray maps visualize time-decoding performance: each pixel's value represents the probability of a timebin #j being decoded as #i, where i and j are the row and column indices of heatmaps. High classification accuracy is indicated by bright colors on the diagonals such that each 100/250 msec can be recovered exactly.

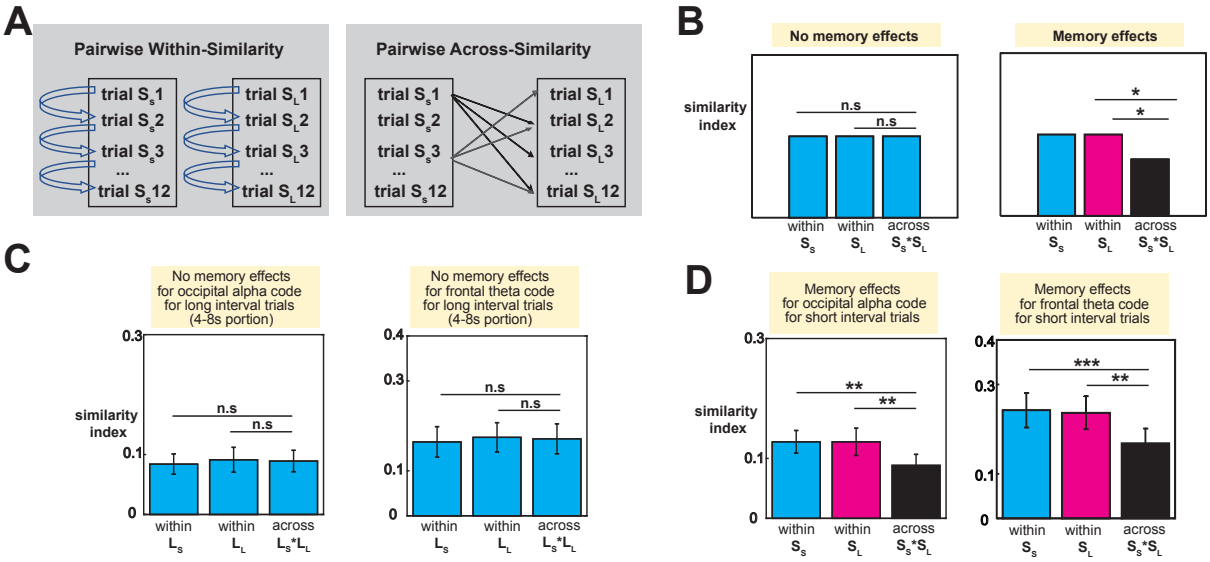

Figure 5. Memory effects on the neural codes of short interval trials. **(a)** Schematics of calculating pairwise within-similarity and cross-similarity indices. **(b)** Hypothetically, null memory effects for short interval trials would predict the equality among three similarity indices: similarity within S_S, similarity within S_L, and similarity across S_S and S_L. The presence of memory effects would predict an inequality. **(c)** For long interval trials (4-8s portion), no memory effects were found for the frontal theta and occipital alpha codes. **(d)** For short interval trials, memory effects were observed for the frontal theta and occipital alpha codes. **Notes**: For the purpose of simplicity, we abbreviate short trials with a previous short trial to S_S, short trials with a previous long trial to S_L, long trials with a previous short trial to L_S, and long trials with a previous long trial to L_L. Error bars represent standard errors. *: $p < 0.05$, **: $p < 0.01$, ***: $p < 0.001$.

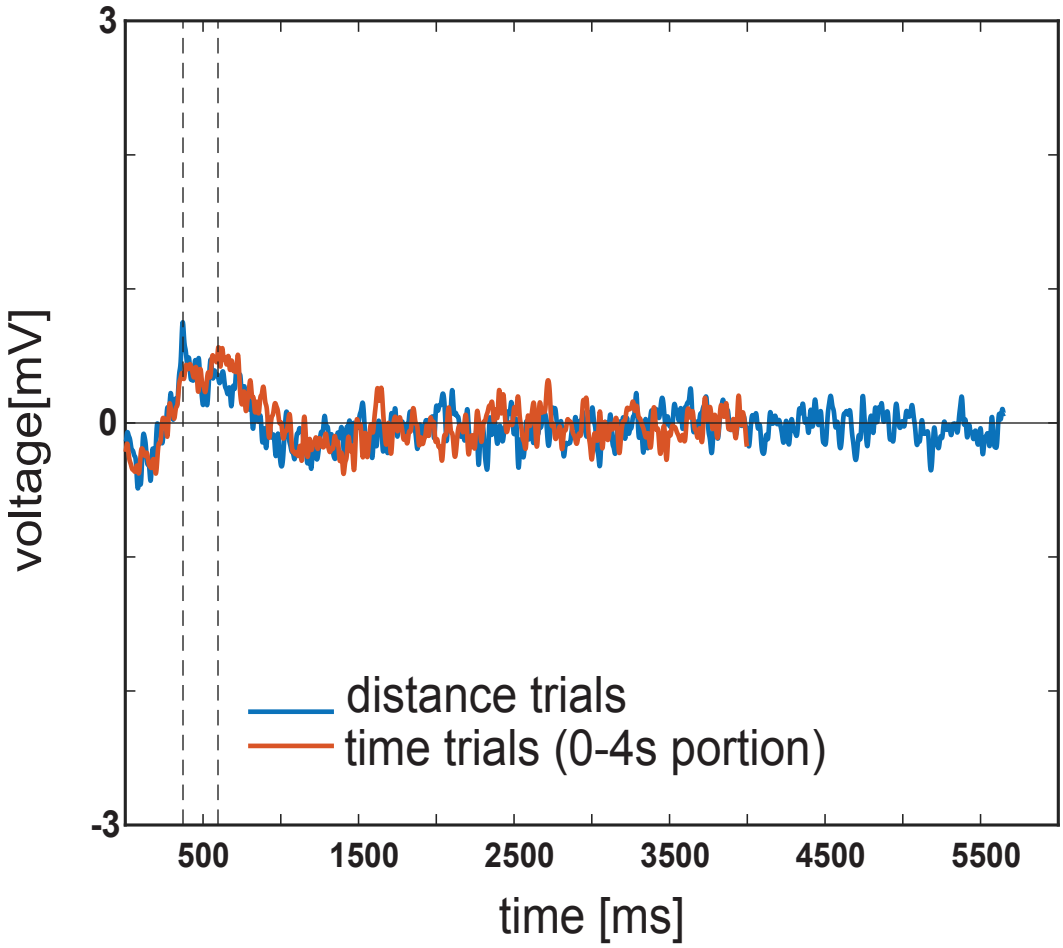

Figure 6. P300-like responses by averaging across trials and participants. The orange line shows the grand P300 from the temporal task (0-4s portion), and the blue line shows the P300 from the spatial task.